doi:10.1006/jmbi.2000.3691 available online at http://www.idealibrary.com on IDEAL® *J. Mol. Biol.* (2000) **298**, 539–555

JMB

Probing Non-Selective Cation Binding in the Hairpin Ribozyme with Tb(III)

Nils G. Walter*, Ning Yang and John M. Burke*

Markey Center for Molecular Genetics, Department of Microbiology and Molecular Genetics, The University of Vermont, 306 Stafford Hall Burlington, VT 05405, USA

*Corresponding authors

Catalysis by the hairpin ribozyme is stimulated by a wide range of both simple and complex metallic and organic cations. This independence from divalent metal ion binding unequivocally excludes inner-sphere coordination to RNA as an obligatory role for metal ions in catalysis. Hence, the hairpin ribozyme is a unique model to study the role of outer-sphere coordinated cations in folding of a catalytically functional RNA structure. Here, we demonstrate that micromolar concentrations of a deprotonated aqueous complex of the lanthanide metal ion terbium(III), $Tb(OH)(aq)^{2+}$, reversibly inhibit the ribozyme by competing for a crucial, yet non-selective cation binding site. $Tb(OH)(aq)^{2+}$ also reports a likely location of this binding site through backbone hydrolysis, and permits the analysis of metal binding through sensitized luminescence. We propose that the critical cation-binding site is located at a position within the catalytic core that displays an appropriately-sized pocket and a high negative charge density. We show that cationic occupancy of this site is required for tertiary folding and catalysis, yet the site can be productively occupied by a wide variety of cations. It is striking that micromolar $Tb(OH)(aq)^{2+}$ concentrations are compatible with tertiary folding, yet interfere with catalysis. The motif implicated here in cation-binding has also been found to organize the structure of multi-helix loops in evolutionary ancient ribosomal RNAs. Our findings, therefore, illuminate general principles of non-selective outer-sphere cation binding in RNA structure and function that may have prevailed in primitive ribozymes of an early ''RNA world''.

Keywords: footprinting; hairpin ribozyme; lanthanide fluorescence; non-specific metal ion binding; outer-sphere cation binding pocket

Introduction

The discovery of catalytic function in certain RNAs, termed ribozymes, spurred great interest in the underlying reaction mechanisms (Cech, 1993; Narlikar & Herschlag, 1997; Been & Wickham, 1997; Sigurdsson *et al.*, 1998; Wedekind & McKay, 1998; Walter & Burke, 1998). Divalent metal ions were soon identified as essential cofactors for catalysis, and ribozymes were generally described as metalloenzymes (Pan *et al.*, 1993; Yarus, 1993; Steitz & Steitz, 1993; Smith, 1995; Pyle, 1993, 1996). Divalent metal ions are thought to play two major roles in RNA catalysis: (1) an indirect role, in which they fold a functional RNA structure by neutralizing and bridging the negatively charged phosphoribose backbone; and (2) a direct role in reaction chemistry, presumably activating reactants by Lewis-acid type inner-sphere coordination. These two roles have proven difficult to dissect.

Recently, the hairpin ribozyme has been found to maintain high levels of site-specific cleavage activity independent of divalent metal ions, in the presence of the kinetically inert metal ion complex cobalt(III) hexammine (Hampel & Cowan, 1997; Nesbitt *et al.*, 1997; Young *et al.*, 1997), high monovalent cation concentrations (Murray *et al.*, 1998; Nesbitt *et al.*, 1999), or organic polyamines such as spermine (Earnshaw & Gait, 1998). These findings unequivocally exclude inner-sphere coordination to RNA as an obligatory role for metal ions in catalysis. Hence, the hairpin ribozyme can serve as a

Present address: N. G. Walter, Department of Chemistry, University of Michigan, Ann Arbor, MI 48109-1055, USA.

Abbreviations used: FRET, fluorescence resonance energy transfer.

E-mail addresses of the corresponding authors: nwalter@umich.edu; jburke@zoo.uvm.edu

0022-2836/00/030539–17 $30.00/0

model to understand the role of a variety of outer-sphere coordinated cations in folding of a catalytically functional RNA structure, independent of any direct involvement in reaction chemistry.

Several ribozymes share this unexpected lack of selectivity in cation cofactor, including the hammerhead and VS ribozymes (Murray *et al*., 1998), as well as RNA and DNA enzymes found through *in vitro* selection from random pools (Geyer & Sen, 1997; Faulhammer & Famulok, 1997; Jayasena & Gold, 1997; Suga *et al*., 1998). In all of these cases, the catalytic motifs are small (30-150 nt), and catalysis comprises a relatively simple, albeit specific nucleophilic substitution reaction, typically a phosphodiester transfer. Larger ribozymes with a more complex function, such as group I and group II introns or RNase P RNA, require more specific metal ion cofactors (Celander & Cech, 1991; Smith *et al*., 1992; Cate *et al*., 1996, 1997; Cate & Doudna, 1997; Basu *et al*., 1998). These observations raise the possibility that primitive catalytic RNAs with non-selective metal-ion binding sites may have emerged first in an ''RNA world'', subsequently evolving into larger catalysts with the ability to bury specific metal ions in their complex tertiary structure, exploiting them for more elaborate tasks (Feig & Uhlenbeck, 1999). Studying the hairpin ribozyme with its broad cofactor spectrum, therefore, may allow a glimpse at the non-selective outer-sphere cation-binding sites of primitive ribozymes at the early stages of life.

The hairpin ribozyme is found in satellite RNAs associated with plant viruses such as the tobacco ringspot virus (Buzayan *et al*., 1986; Hampel & Tritz, 1989). These virus satellites proliferate by recruiting the viral replicase for a double rolling-circle replication of their circular positive-strand RNA genome. The hairpin ribozyme motif is required for self-cleavage and ligation of the replicated negative-strand polymers into cyclic monomers that can serve as templates in positive-strand synthesis. In its natural configuration, the hairpin ribozyme is embedded in an RNA four-way junction, that can be truncated into a hinged two-way junction to reversibly cleave a substrate *in trans* (Hampel & Tritz, 1989). The two essential domains contribute determinants for substrate binding (domain A) and catalysis (domain B). Both domains fold independently, each forming a highly conserved internal loop flanked by two helices (Figure 1(a)) (Walter & Burke, 1998). Site-specific substrate cleavage and ligation reactions require loops A and B to interact, and this docking event involves a sharp bend about the interdomain junction (Walter & Burke, 1998). The natural four-way junction serves as scaffold to stabilize docking of the two domains (Walter *et al*., 1999), presumably recruiting two multivalent metal ions, at least one of which binds at the helical junction (Murchie *et al*., 1998). As activity requires higher metal ion concentrations than docking, yet another, lower-affinity metal-ion binding site has been proposed to be essential for activity of the four-way junction ribozyme (Thomson & Lilley, 1999).

In the two-way junction ribozyme, domain docking and cleavage activity show parallel metal ion dependencies (Walter *et al*., 1998, 1999), suggesting that the same lower-affinity metal ion binding event is responsible for both. As this junction design is extensively used for targeted RNA inacti-

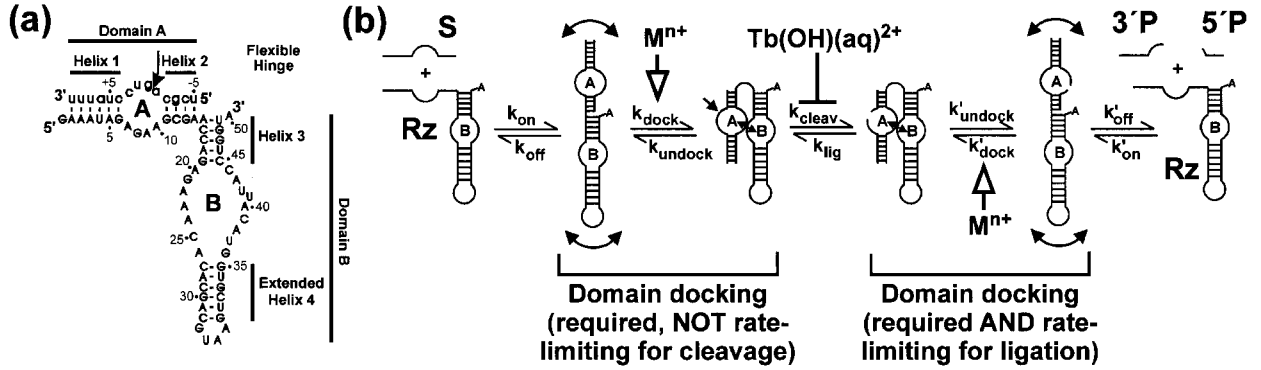

Figure 1. The hairpin ribozyme and its reaction pathway. (a) Ribozyme-substrate complex. The kinetically optimized construct SV5 EH4 Rz from Esteban *et al*. (1997) was used throughout this study. The ribozyme (capital letters) binds the 14-nucleotide substrate (small letters) through its substrate-binding strand to form domain A. Domain A is connected *via* a flexible hinge to domain B of the ribozyme which contributes essential catalytic determinants. Both domains are characterized by a highly conserved internal loop with flanking Watson-Crick base-paired helices. The arrow indicates the cleavage site. (b) Minimal reaction pathway of hairpin ribozyme catalysis, as derived previously (Walter *et al*., 1998). Substrate *in trans* (S) is bound by the ribozyme (Rz) into an open (extended) conformation. This structural isomer is flexible (curved double arrows) and, upon addition of cation M^{n+}, folds into a bent (docked) structure, enabling loops A and B to interact (short double arrow). Subsequently, site-specific cleavage occurs (short arrow), the complex undocks, and the 5′ and 3′ cleavage products (5′P, 3′P) dissociate. All steps are reversible and can be characterized by individual rate constants as indicated. Domain docking was found to be rate-limiting for ligation, but not cleavage, where a subsequent, more local conformational change might be the slowest step (Walter *et al*., 1998). In the present work, we investigate the interference of micromolar concentrations of the deprotonated complex $Tb(OH)(aq)^{2+}$ with a post-docking step.

vation in mammalian cells (Welsh *et al*., 1996; Earnshaw & Gait, 1997), there is considerable interest in understanding the mechanism of substrate cleavage. We have used fluorescence based kinetic assays to dissect the reaction pathway into several conformational transitions (Walter & Burke, 1997; Walter *et al*., 1998). Domain docking was found to be an essential global folding step, preceding the rate-limiting event in catalysis (Figure 1(b)) (Walter *et al*., 1998). As the observed cleavage rate is pH independent (Nesbitt *et al*., 1997), and since docked ribozyme-substrate and ribozyme-product complexes show the same solvent protected core (Hampel *et al*., 1998), the rate-limiting step may well be a localized conformational transition following docking.

Recently, the solution structures of the isolated domains A and B of the ribozyme-substrate complex have been determined by NMR (Cai & Tinoco, 1996; Butcher *et al*., 1999). NMR spectra were obtained, however, at low ionic strength, in the absence of multivalent cations. Since domain docking is not detectable under these conditions (Walter *et al*., 1998, 1999; Hampel *et al*., 1998), it seems reasonable to assume that multivalent metal ion binding has an impact on these structures in a manner to favor interdomain interactions. Recently, a molecular model of these interactions, implementing a ''ribose zipper'' motif, was proposed based on cross-linking interference experiments (Earnshaw *et al*., 1997; Pinard *et al*., 1999a). However, we have evidence for a more intimate ''induced fit'' between loops A and B in the catalytic core of the hairpin ribozyme-substrate complex as a prerequisite for site-specific substrate cleavage (Pinard *et al*., 1999b).

Here, we have characterized the lanthanide metal ion terbium(III) as a potent inhibitor of catalysis by the hairpin ribozyme. It functions as a competitive inhibitor for all cations known to promote activity, reversibly blocking a step in the reaction pathway following domain docking, possibly the rate-limiting step. As inhibition is strongly pH dependent, only the deprotonated complex $Tb(OH)(aq)^{2+}$ appears to inhibit. We were also able to identify a high affinity binding site of $Tb(OH)(aq)^{2+}$ in the catalytic core of the ribozyme by a slow backbone scission reaction, and propose that this site is a likely candidate for inducing the observed inhibition. In the NMR structure of loop B, this non-selective binding pocket for cations is located in a region of high negative surface charge potential.

Results

Terbium(III) inhibits the hairpin ribozyme by competing with all cations that support catalysis

Terbium(III) is the most stable oxidation state of the eighth of the twelve lanthanide transition metals. It has been used, together with europium(III), as a probe for binding sites of metal ions, particularly Mg^{2+} and Ca^{2+}, in protein enzymes (Horrocks *et al*., 1977; Evans, 1990; Horrocks, 1993; Frey *et al*., 1996; Dickeson *et al*., 1998). Other lanthanide ions, in particular samarium(III) and luthetium(III), have been used to solve the phase problem in X-ray diffraction analysis of tRNA crystals, by providing isomorphic heavy-atom derivatives (Jack *et al*., 1977). They were found to often bind to sites on RNA identical with Mg^{2+}-binding sites. More recent studies have shown that terbium(III) (Feig *et al*., 1998) and lanthanum(III) (Lott *et al*., 1998) interfere with activity of the hammerhead ribozyme, by competing with Mg^{2+} binding. These results prompted us to investigate the impact of terbium(III) on hairpin ribozyme activity to better understand the role of metal ions in catalysis by RNA.

For activity interference studies we employed a structurally well-behaved and kinetically well-characterized variant of the hairpin ribozyme (SV5 EH4 Rz as described by Esteban *et al*. (1997); Figure 1(a)). This construct has been shown to form a stably docked conformational intermediate before proceeding to the rate-limiting step of catalysis (Walter *et al*., 1998, 1999). Ribozyme and radiolabeled substrate were combined under single-turnover (pre-steady-state) conditions (ribozyme excess) at pH 7.5, in the presence of 200 mM Na^{+}, to ensure that all substrate strands were incorporated into yet inactive complexes. Cleavage was initiated by the addition of a mixture of terbium(III) and a second, catalytically proficient cation. Cleavage rate constants were determined using standard methods (see Materials and Methods), and their normalized values were plotted as inhibition or activation curves over a range of cation concentrations (Figure 2). Results show that terbium(III) is an efficient inhibitor of all cations that support catalysis, including the hard and soft divalent metal ions magnesium (Mg^{2+}) and manganese (Mn^{2+}), respectively, the kinetically inert trivalent metal ion complex cobalt(III) hexammine ($Co(NH_3)_6^{3+}$), the organic triamine spermidine (spd^{+++}), and the monovalent metal ion sodium (Na^{+}) (Figure 2, left panel). The observed inhibition constants $K_{i,app}$ under the chosen conditions are in the narrow range of 12 to 33 μM. In all cases, terbium(III)-mediated inhibition can be reversed by increasing the concentration of the catalytically proficient cation, and the apparent binding constant $K_{D,app}$ for the cation is higher in the presence than in the absence (value in parenthesis) of terbium(III) (Figure 2, right panel). These observations strongly suggest a competition between terbium(III) and the catalytically proficient cations for a common binding site. Consistent with this notion, activity in a reaction stalled in the presence of 12 mM Mg^{2+} and 50 μM terbium(III) could partially be rescued by subsequently increasing the Mg^{2+} concentration to 500 mM (data not shown).

Apparent cooperativity coefficients for terbium(III) are high (Figure 2), presumably indicative of

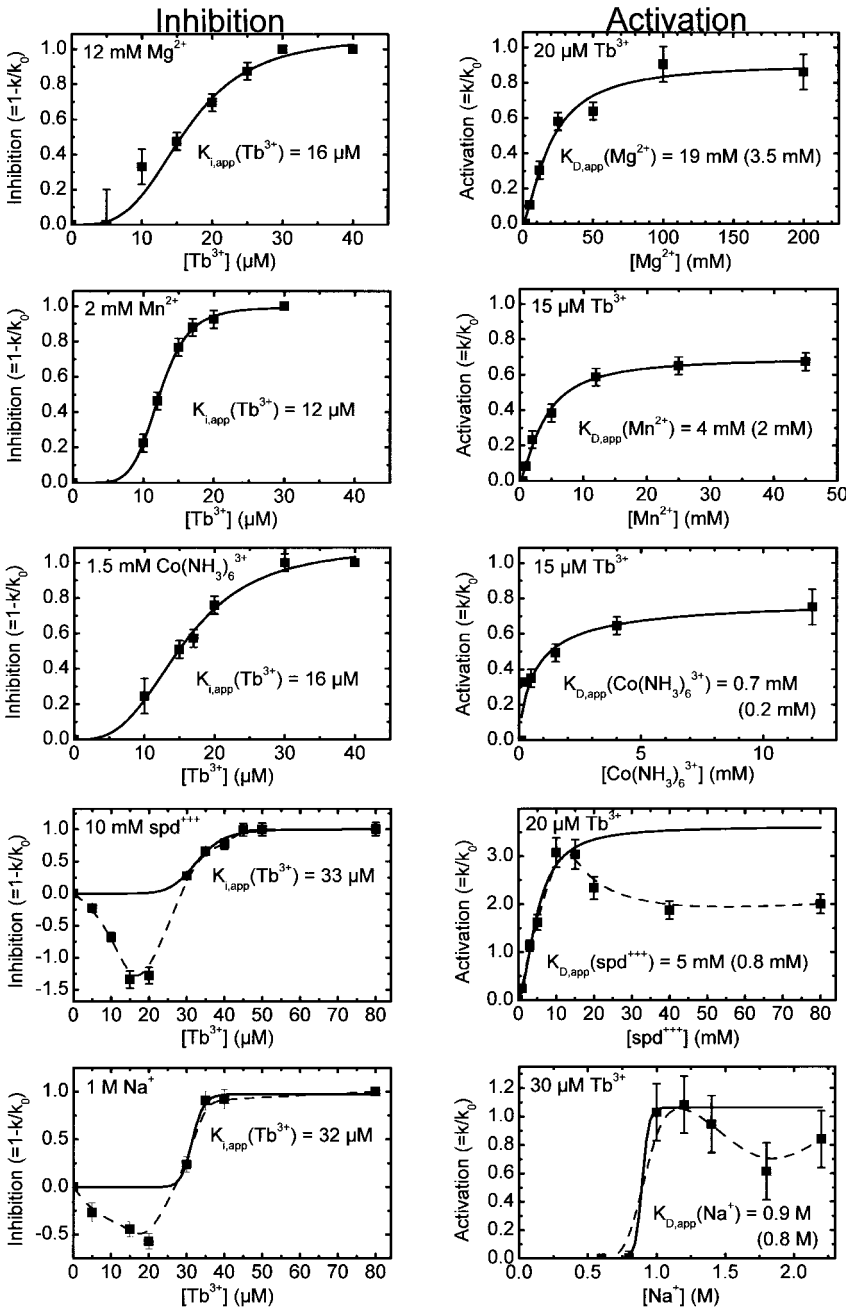

Figure 2. Inhibition of hairpin ribozyme cleavage activity by terbium(III). Substrate and ribozyme were annealed under single-turnover conditions at 25 °C in 100 mM Tris-HCl (pH 7.5), in a background of 200 mM Na^+ to ensure proper secondary structure formation. Terbium(III) and the catalytically proficient cation were subsequently added together; the constant cation component is stated on each plot. k and k_0 are the average rate constants in the presence and absence of terbium(III), respectively. Data were fitted with cooperative binding equations (continuous lines) to yield the indicated apparent binding constants $K_{i,app}$ and $K_{D,app}$ (see Materials and Methods). B-spline interpolations of the data points, broken lines. (Left panel) Inhibition curves with increasing terbium(III) concentration. k_0 was 0.088 min^{-1}, 0.053 min^{-1}, 0.084 min^{-1}, 0.018 min^{-1}, and 0.039 min^{-1} for 12 mM Mg^{2+}, 2 mM Mn^{2+}, 1.5 mM $Co(NH_3)_6^{3+}$, 10 mM spd^{+++}, and 1 M Na^+, respectively. Apparent cooperativity coefficients were 3.5 (Mg^{2+}), 6.0 (Mn^{2+}), 3.0 ($Co(NH_3)_6^{3+}$), 9.0 (spd^{+++}), and 21 (Na^+), respectively. (Right panel) Re-activation curves with increasing cation concentrations. Apparent cooperativity coefficients were 1.4 (Mg^{2+}), 1.4 (Mn^{2+}), 0.8 ($Co(NH_3)_6^{3+}$), 3.6 (spd^{+++}), and 38 (Na^+), respectively. Note that the reported data are convoluted (see Materials and Methods), so that high apparent cooperativity coefficients are unlikely to correlate with terbium(III) stoichiometry.

a narrow binding range for terbium(III) rather than a stoichiometry. It is striking that in the presence of 10 mM spermidine or 1 M Na^+, low concentrations of terbium(III) actually enhance activity (negative inhibition values); inhibition is only observed at concentrations above 30 µM (Figure 2, left panel). Likewise, in the corresponding reverse titrations, activity at intermediate spermidine or Na^+ concentrations and a fixed terbium(III) concentration can exceed that in the absence of terbium(III) (activation values >1). Increasing the cation concentration further leads to a decrease in activation (Figure 2, right panel). This behavior is not observed with the other cations tested and suggests that: (1) terbium(III) is not necessarily detrimental for hairpin ribozyme activity; (2) terbium(III) and monovalent cations might play complementary and synergistic roles in the observed activation; and (3) there may be multiple binding sites and/or terbium(III) species involved in the observed inhibition/activation effects.

Reversible inhibition by the deprotonated species $Tb(OH)(aq)^{2+}$

In solution, lanthanide(III) metal ions readily produce a mixture of mono- and polynuclear hydroxo complexes (Baes & Mesmer, 1976; Matsumura & Komiyama, 1997). For terbium(III), the hydrolysis:

$$Tb(aq)^{3+} \rightleftharpoons Tb(OH)(aq)^{2+} + H^+$$

has an equilibrium constant of $K_{eq} = 10^{-7.9}$ M (at low ionic strength) and yields significant amounts of the deprotonated mononuclear species $Tb(OH)(aq)^{2+}$ at pH 7.5 (Baes & Mesmer, 1976). From this intermediate, other species such as $Tb(OH)_2(aq)^{+}$, $Tb_2(OH)_2(aq)^{4+}$, or $Tb_3(OH)_5(aq)^{4+}$ can form, ultimately leading to the precipitation of terbium hydroxide, $Tb(OH)_3$, at high pH and terbium(III) concentrations. In the handling of our solutions, we carefully avoided formation of any hydroxide precipitate (see Materials and Methods). However, it seemed important to determine which of the soluble hydroxo complex(es) mediates inhibition, and whether the various terbium(III) complexes in solution might have distinct effects on hairpin ribozyme activity, a possibility raised by our experiments with monovalent cations (see above).

Decreasing pH from 7.5 to 6.5 had a dramatic effect on terbium(III)-mediated inhibition (Figure 3(a)); in the presence of 12 mM Mg^{2+}, addition of 20 to 100 μM terbium(III) now enhances activity nearly threefold. However, at concentrations of 300 μM and above, complete inhibition was observed, as before. Terbium(III) can also promote hairpin ribozyme activity in the

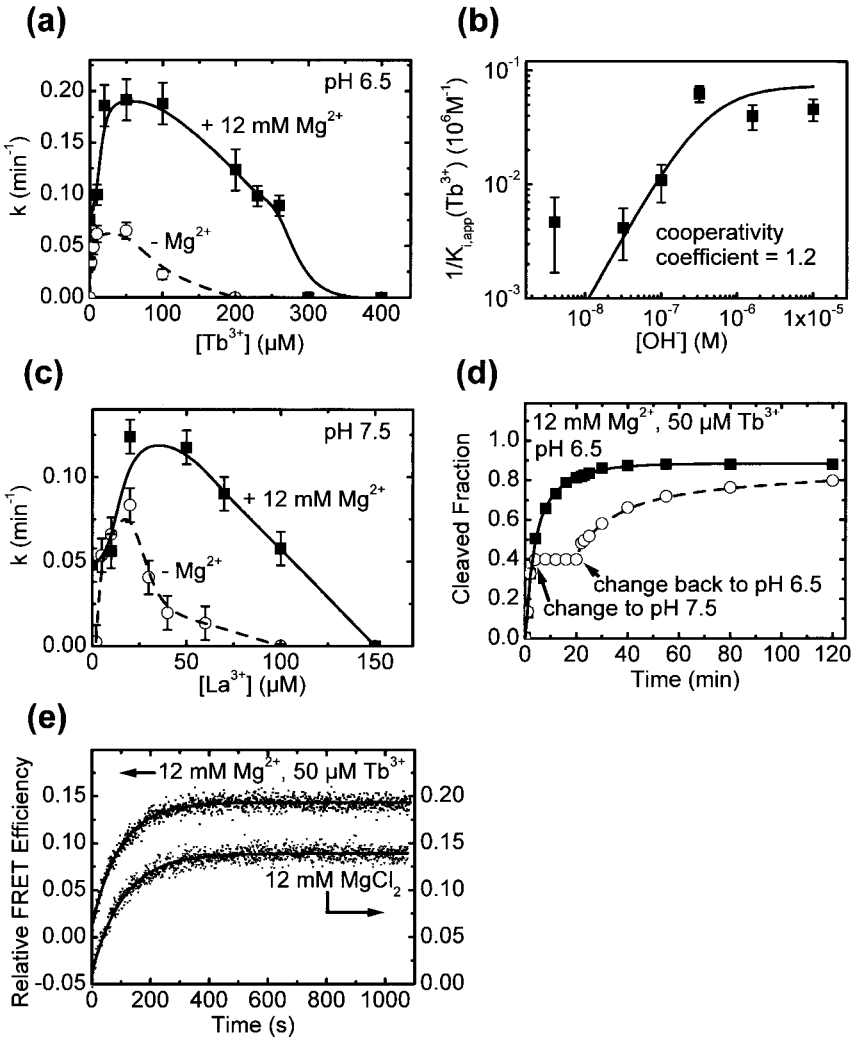

Figure 3. Properties of terbium(III)-mediated inhibition of the hairpin ribozyme at 25 °C. (a) Rate constants k (see Materials and Methods) with increasing terbium(III) concentration at pH 6.5 in the presence (filled squares, continuous line) and absence (open circles, broken line) of 12 mM Mg^{2+}. Lines represent B-spline interpolations of data points. In the presence of Mg^{2+}, an inhibition constant for terbium(III) of 240 μM can be calculated from the data (see Materials and Methods). (b) Dependence of the inverse of the apparent inhibition constant of terbium(III) on hydroxide ion concentration in the presence of each 12 mM Mg^{2+} and terbium(III). Non-linear regression (continuous line) using the cooperativity equation (see Materials and Methods) yields a cooperativity coefficient of close to 1, and an apparent $K_D^{OH^-}$ of $10^{-6.4}$ M (equivalent to a titration midpoint at pH 7.6). (c) Average rate constants k (see Materials and Methods) with increasing lanthanum(III) concentration at pH 7.5 in the presence (filled squares, continuous line) and absence (open circles, broken line) of 12 mM Mg^{2+}. Lines represent B-spline interpolations of data points. In the presence of Mg^{2+}, an inhibition constant for lanthanum(III) of 97 μM can be calculated from the data. (d) Terbium(III)-mediated inhibition is reversible. Two parallel reactions were initiated by the addition of 12 mM Mg^{2+} and 50 mM Tb^{3+}, at pH 6.5, resulting in rapid accumulation of cleavage product (see also (a)). One reaction (open circles, broken line) was subjected to a change in pH to 7.5, completely stalling catalysis (see also Figure 2). After 20 minutes conditions were changed back to pH 6.5, and catalysis resumed to similar levels as the reference reaction (filled squares, continuous line). B-spline interpolations of data points, lines. (e) Terbium(III) does not interfere with domain docking. At conditions of terbium(III)-mediated inhibition of cleavage (12 mM Mg^{2+}, 50 μM Tb^{3+} (pH 7.5); see also Figure 2) a fluorescence resonance energy transfer (FRET) assay (Walter *et al.*, 1998) (see Materials and Methods) reveals the same level of domain docking (monitored as increase in relative FRET efficiency) in the ribozyme-substrate (dA_{-1} analog) complex as does a reference reaction in the absence of Tb^{3+}. Continuous lines represent single-exponential fits to the data points, yielding docking rate constants k_{dock} of 0.63 min^{-1} and 0.55 min^{-1} and identical amplitudes in the presence and absence of terbium(III), respectively.

absence of Mg^{2+} at pH 6.5, with a similar asymmetric bell-shaped concentration dependence as in the presence of Mg^{2+} (Figure 3(a)).

Determining the apparent inhibition constant $K_{i,app}$ over a range of hydroxide ion concentrations yields a cooperativity coefficient with respect to OH^- close to 1 and a titration midpoint of pH 7.6 (Figure 3(b)). Both values strongly suggest that inhibition is mediated by the most prevalent species in solution, $Tb(OH)(aq)^{2+}$, as this complex contains one OH^- ligand with a titration midpoint of pH 7.9 (see above).

To further test this hypothesis, we examined lanthanum(III) as a potential inhibitor of the hairpin ribozyme. As the first in the row of lanthanide ions, lanthanum(III) has a slightly larger ionic radius than terbium(III) (1.15 Å, compared to 0.92 Å). As a result, it has a slightly higher hydrolysis equilibrium constant of $K_{eq} = 10^{-8.5}$ M (at low ionic strength) and is fourfold less deprotonated at pH 7.5 than terbium(III). Accordingly, hairpin ribozyme activity showed a bell-shaped dependence on lanthanum(III) concentration at pH 7.5, both in the presence and absence of Mg^{2+} (Figure 3(c)), similar to the curves observed for terbium(III) at pH 6.5 (Figure 3(a)). The apparent inhibition constant for lanthanum(III) in the presence of 12 mM Mg^{2+} is sixfold higher than that of terbium(III) at the same pH (97 μM *versus* 16 μM), in reasonable agreement with their difference in deprotonation equilibrium, and consistent with $La(OH)(aq)^{2+}$ as the inhibitory species. As an enhancement of hairpin ribozyme activity is only seen at low pH, it seems likely that the activation by low concentrations of either terbium(III) (pH 6.5 or below) or lanthanum(III) (pH 7.5) is mediated by the fully protonated aqueous complexes $Tb(aq)^{3+}$ and $La(aq)^{3+}$, respectively.

This strong effect of pH on the inhibition by terbium(III) allows for a simple reversibility test. Two parallel reactions were initiated at pH 6.5, in the presence of 12 mM Mg^{2+} and 50 μM terbium(III), leading to the rapid accumulation of cleavage product. After two minutes, the pH of one of the two reactions was changed to 7.5, completely suppressing cleavage. After 20 minutes, this reaction was brought back to pH 6.5, resulting in the recovery of cleavage activity to similar extents as the control reaction (Figure 3(d)) and proving that inhibition indeed is readily reversible.

What is the mode of action for terbium(III)-mediated reversible inhibition of the hairpin ribozyme? Terbium(III) at low concentrations has previously been found to alter the geometry of the sugar-phosphate backbone and the base stacking interactions in nucleic acids (Gersanovski *et al*., 1985). This interference can be expected to be reversible and has the potential to impair essential structural transitions in the reaction pathway of a catalytic RNA. Under our experimental conditions, the hairpin ribozyme-substrate complex is formed prior to the addition of terbium(III). A subsequent and essential structural transition of the complex is known to involve folding from an extended to a docked conformation, in which the substrate-binding and catalytic domains interact, enabling catalysis (Figure 1(b)) (Walter *et al*., 1998, 1999; Hampel *et al*., 1998). A convenient way to monitor this global folding event is as an increase in fluorescence resonance energy transfer (FRET) between a domain-terminal donor/acceptor fluorophore pair (Walter *et al*., 1998). Figure 3(e) shows a comparison of FRET-monitored domain docking in the presence and absence of 50 μM terbium(III), a concentration sufficient to completely stall cleavage activity under these conditions (12 mM Mg^{2+}, pH 7.5). Clearly, formation of the docked conformer is not inhibited by the presence of terbium(III), suggesting that the mechanism of inhibition involves a step after domain docking and, hence, closer to the chemical transition state (Figure 1(b)). This result was confirmed at terbium(III) concentrations of up to 100 μM (above which the FRET donor fluorescein becomes strongly quenched by terbium(III)) and by mapping the solvent-protected core of the ribozyme-substrate complex in the presence and absence of terbium(III), employing hydroxyl radical footprinting (Hampel *et al*., 1998; Ken J. Hampel, personal communication).

Energy transfer from RNA bases enables monitoring terbium(III) binding to the hairpin ribozyme-substrate complex

Terbium(III) has been known to bind to RNA and, as a result, to fluoresce upon excitation of the RNA, through energy transfer particularly from nearby guanine bases (Yonushot *et al*., 1978; Topal & Fresco, 1980; Wenzel & Collette, 1988). We found that this effect can be used to monitor the kinetics and thermodynamics of terbium(III) binding to the hairpin ribozyme-substrate complex in a background of 12 mM Mg^{2+}. Figure 4(a) shows the strong enhancement of the fluorescence emission spectrum of terbium(III) by addition of the RNA complex. In a stopped-flow kinetic experiment, the rapid binding of a millimolar excess of terbium(III) to micromolar RNA concentrations can be resolved into at least three different processes with discernable rate constants of 41 s^{-1}, 2.9 s^{-1}, and 0.25 s^{-1} (Figure 4(b)). 66 % of the fluorescence increase is associated with the fastest rate, suggesting that binding is driven by electrostatic attraction of terbium(III) cations to areas on the RNA with high negative charge potential.

An equilibrium titration of the ribozyme-substrate complex with terbium(III) in 12 mM Mg^{2+} indicates at least three distinct classes of binding sites with affinities of 9 μM, 120 μM, and 900 μM, respectively (Figure 4(c)), similar to previous observations on lanthanide(III) ion binding to tRNA (Draper, 1985). Note that the highest affinity binding is observed at similar concentrations as the inhibition of ribozyme activity ($K_{i,app} = 16$ μM under these conditions, see Figure 2).

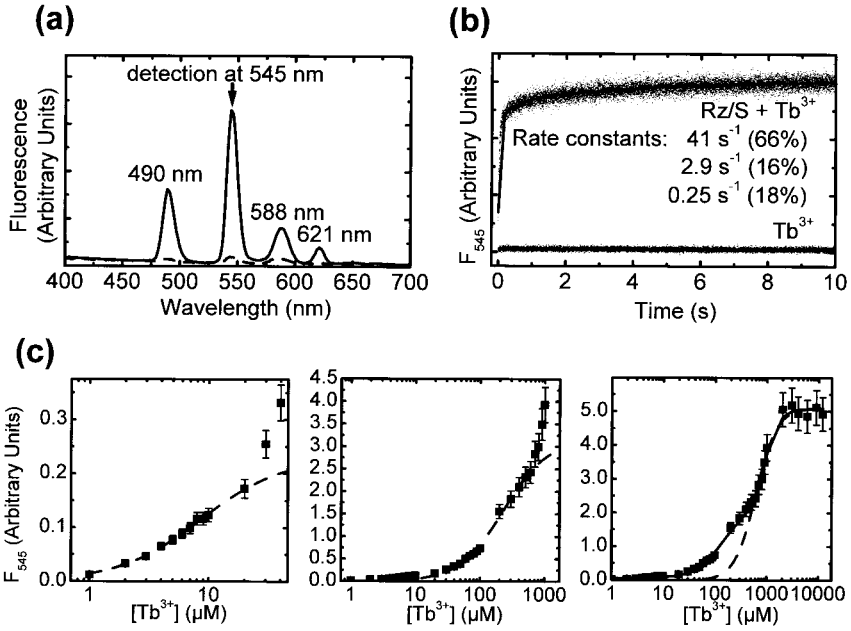

Figure 4. Fluorescence detection of terbium(III) binding to the hairpin ribozyme-substrate complex in 50 mM Tris-HCl (pH 7.5), 12 mM Mg^{2+}, at 25 °C. (a) When excited at 290 nm, 2 mM terbium(III) bound to 1 μM ribozyme-substrate complex (dA_{-1} analog) exhibits a characteristic fluorescence spectrum (continuous line). In the absence of RNA, only a low background signal is observed (broken line). (b) In a stopped-flow fluorescence experiment (1 datum per millisecond; excitation, 290 nm; emission detection: 545 nm; 29 individual time traces averaged), the binding kinetics of 2 mM terbium(III) to 1 μM ribozyme-substrate complex (dA_{-1} analog) reveal at least three separate rate constants (relative amplitudes in parenthesis; fit: continuous line), not seen in the absence of RNA. (c) Binding of terbium(III) to 1 μM ribozyme-substrate complex (dA_{-1} analog) can be monitored by fluorescence titration over several orders of magnitude of terbium(III) concentration (excitation, 290 nm; emission detection, 545 nm). Fits assuming a single binding affinity (broken lines) accurately represent the data only in narrow concentration ranges. The best fit to the complete data set (continuous line in right panel) was obtained when fitting to the sum of three independent Hill equations (see Materials and Methods), revealing apparent dissociation constants of 9 μM, 120 μM, and 900 μM.

Terbium(III) at millimolar concentrations footprints RNA secondary and tertiary structure, while micromolar concentrations report only on the tightest binding site

Terbium(III), like other lanthanide and heavy-metal ions such as lead, has been used to detect specific metal-ion binding sites in RNA (Jack *et al.*, 1977; Ciesiolka *et al.*, 1989; Evans, 1990; Gast *et al.*, 1996; Feig & Uhlenbeck, 1999) or to degrade RNA for biotechnological applications (Stein & Cohen, 1988; Morrow, 1996; Matsumura & Komiyama, 1997), taking advantage of a metal-ion-promoted hydrolytic backbone scission reaction. We found that high (12 mM) concentrations of terbium(III) produce a clear footprinting pattern of the secondary and tertiary structure of (5′-^{32}P)-labeled hairpin ribozyme. Under these conditions, terbium(III) cleaves the RNA backbone in a sequence-independent manner, preferentially cutting single-stranded or non-Watson-Crick base-paired regions such as loops A and B, or the GNRA tetraloop closing helix 4 of the hairpin ribozyme (Figure 5). We used order-of-addition experiments to characterize this structure probing method.

At low concentrations of terbium(III), the primary scission products co-migrate with the 2′,3′-cyclic phosphate products of the control alkali ladder, while only higher terbium(III) concentrations convert the primary products into the higher-mobility 2′- or 3′-phosphate fragments (best visible by comparing region H1 of lanes 20 to 23 with that of lane ''OH^-'', Figure 5(a)). This observation is consistent with the previously proposed two-step mechanism for metal-ion-promoted RNA backbone scission (Pan & Uhlenbeck, 1992), involving, first, deprotonation of a 2′-hydroxyl group and nucleophilic attack of the resulting oxyanion on the adjacent 3′,5′-phosphodiester to form 2′,3′-cyclic phosphate and 5′-hydroxyl termini, and, second, hydrolysis of the cyclic phosphate to yield the corresponding mixture of 2′- and 3′-phosphomonoesters.

Addition of 12 mM terbium(III) to the hairpin ribozyme prior to addition of substrate produced a footprint similar to that in the absence of substrate (compare lane 7 with lane 6, Figure 5(a)), with the single-stranded substrate-binding strand (comprising regions H1, loop A, and H2) strongly and uniformly hit. Hence, millimolar concentrations of terbium(III) can prevent substrate binding to the hairpin ribozyme. In contrast, when the substrate is allowed to bind before addition of terbium(III), the substrate-binding strand becomes strongly protected from scission, in particular helices H1 and H2 (lane 8, Figure 5(a)). In this case, the footprinting pattern is independent of whether Mg^{2+} is added after or together with terbium(III) (compare lane 8 with lane 9, Figure 5(a)), indicating that high terbium(III) concentrations can interfere with tertiary structure formation of the ribozyme-substrate complex. However, if Mg^{2+} is added before terbium(III) such that the ribozyme-substrate complex is tertiary structure folded when footprinted, the footprinting pattern is very different, demonstrating that terbium(III) does not disrupt a preformed tertiary structure. Under these conditions,

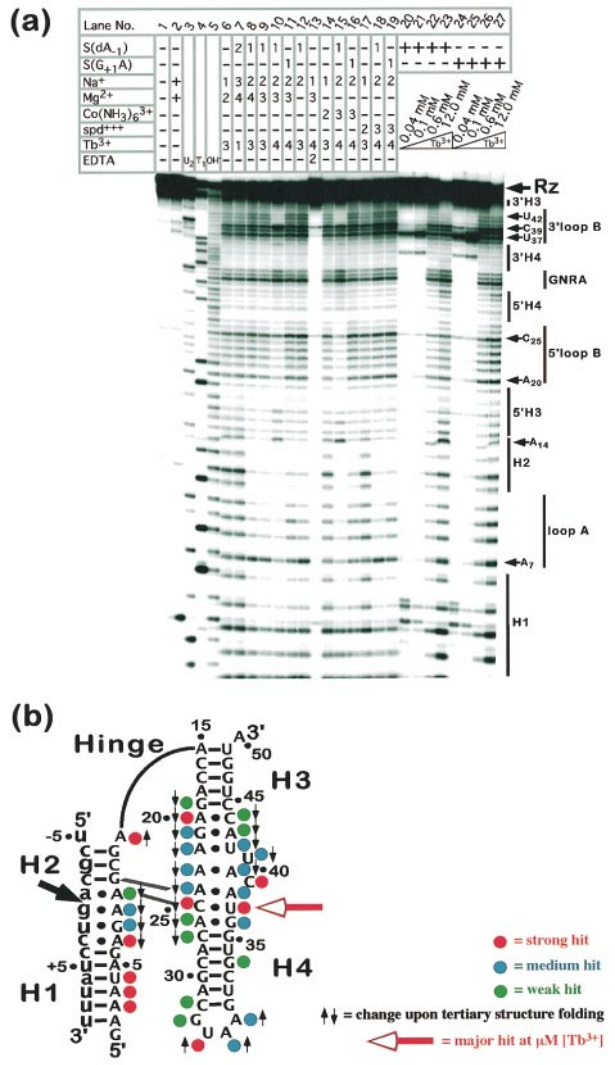

Figure 5. Terbium(III)-mediated footprinting of the hairpin ribozyme. (a) Footprint of (5′-^{32}P)-labeled hairpin ribozyme (Rz) after incubation with terbium(III) over two hours at 25 °C. Lanes 1 and 2, controls; lanes 3 and 4, sequencing ladders with RNase U_2 (cutting after A) and RNase T_1 (cutting after G); lane 5, partial alkali hydrolysis; lanes 6-19, order of addition experiments (numbers indicate order) with a 100-fold excess (500 nM) of non-cleavable substrate analog S(dA_{-1}) or S($G_{+1}A$), 100 mM Na^+, 12 mM Mg^{2+}, 12 mM $Co(NH_3)_6^{3+}$, and 12 mM spermidine (spd^{+++}), 12 mM Tb^{3+}, and 120 mM EDTA as chelator; lanes 20-27, incubation of 10 μM ribozyme-substrate complex, containing trace amounts of radiolabeled ribozyme, in the presence of 12 mM Mg^{2+} with varying concentrations of Tb^{3+}, as indicated, and with either non-cleavable substrate analog S(dA_{-1}) or S($G_{+1}A$). (b) Superposition of backbone scission sites at 12 mM terbium(III) onto a schematic of the tertiary structure model of the ribozyme (Walter & Burke, 1998). Strong, medium, and weak hits, together with changes caused by tertiary structure formation are indicated at the nucleotides 3′ to which the scission occurs, as deduced from quantitative analysis of lanes 8 (footprint of secondary structure) and 10 (footprint of tertiary structure) in (a). The only major hit at sub-millimolar concentrations of terbium(III) is 3′ to U_{37}.

loop A, the 5′-segment and parts of the 3′-segment of loop B become strongly protected from terbium(III)-mediated scission, while A_{14} at the domain hinge and the GNRA tetraloop become more exposed (compare lane 10 with lanes 8 and 9, Figure 5(a)). These changes are strictly dependent on tertiary structure formation, as shown by their loss in the presence of a substrate analog with a $G+1 \rightarrow A$ mutation (S($G_{+1}A$)) (lane 11, Figure 5(a)), that inhibits docking (Walter *et al.*, 1998, 1999; Hampel *et al.*, 1998), or in the absence of Mg^{2+} (lane 12, Figure 5(a)) as an essential cofactor for docking (Walter *et al.*, 1998). Chelation of terbium(III) with EDTA prevents backbone scission, as expected (lane 13, Figure 5(a)).

Similar results were obtained with cobalt(III) hexammine as the metal ion cofactor (lanes 14 through 16, Figure 5(a)); only the docked ribozyme-substrate complex (lane 15) produces the unique footprinting/protection pattern indicative of proper tertiary structure folding, while the undocked complex with the $G_{+1}A$ substrate analog does not (lane 16). Spermidine, despite promoting a significant level of catalytic activity (with only a five times slower rate constant than magnesium, Figure 2), does not lead to a detectable level of docked complex (lanes 17 through 19, Figure 5(a)), consistent with previous findings (Walter *et al.*, 1998). Spermidine shares this behavior with monovalent cations (Murray *et al.*, 1998). Apparently, cleavage can occur in a transiently docked ribozyme-substrate complex (Pinard *et al.*, 1999b).

Our observation, using fluorescence titration (see above), of at least three distinct affinity classes of terbium(III) binding sites prompted us to perform footprinting assays at different terbium(III) concentrations, both with docked (lanes 20 through 23, Figure 5(a)) and undocked (lanes 24 through 27, Figure 5(a)) ribozyme-substrate complexes. Significantly, at 40 μM and 100 μM terbium(III), the only site saturated for backbone scission is at U_{37} in the 3′-segment of loop B of the ribozyme, both with the docked (lanes 20 and 21) and undocked (lanes 24 and 25) ribozyme-substrate complexes, respectively, suggesting a high-affinity metal-ion binding site in that area. In contrast, millimolar concentrations of terbium(III) bind to many additional sites (lanes 22, 23, 26, and 27), generating the observed footprinting patterns.

Figure 5(b) summarizes the footprinting information from quantification of lanes 8 (before tertiary structure folding) and lane 10 (after tertiary structure folding) of the gel in Figure 5(a) on a schematic of the proposed tertiary structure of the hairpin ribozyme-substrate complex (Earnshaw *et al.*, 1997; Walter & Burke, 1998). Terbium(III) strongly cuts non-Watson-Crick base-paired regions of the ribozyme. Upon tertiary structure folding, several regions, that coincide with regions protected from hydroxyl radical footprinting (Hampel *et al.*, 1998), become partially protected from terbium(III)-mediated backbone scission. By contrast, the backbone of A_{14} at the hinge between

domains A and B becomes more exposed, indicating its role as an extended linker for proper alignment of the two domains (Earnshaw *et al.*, 1997). Overall, the information from footprinting at millimolar concentrations of terbium(III) strongly supports the previously proposed tertiary structure model of the hairpin ribozyme-substrate complex.

A high-affinity, but non-specific outer-sphere terbium(III) binding site is located in the catalytic core of the hairpin ribozyme

It is striking that micromolar concentrations of terbium(III) only saturate a single (high-affinity) scission site in the catalytic core, 3′ to U_{37}, of both the docked and undocked hairpin ribozyme-substrate complexes. This site coincides with the only region in the catalytic core of the ribozyme that does not become protected from terbium(III) footprinting (at millimolar [Tb^{3+}]) upon tertiary structure folding (Figure 5(b)) and, hence, remains solvent-accessible throughout the reaction pathway (Figure 1(b)). Can binding of micromolar terbium(III) to this site directly be correlated with the observed inhibition of catalytic activity at similar terbium(III) concentrations?

To test this hypothesis, we investigated the properties of site-specific scission 3′ to U_{37} (Figure 6). This site is not only saturated at similar concentrations as catalytic inhibition, but like inhibition, backbone scission is suppressed both by increasing Mg^{2+} and cobalt(III) hexammine concentration (Figure 6(a) and (b)). A plot of the scission rate constant over increasing terbium(III) concentrations yields a cooperativity coefficient below 1, suggesting the involvement of a mononuclear terbium(III) complex (Figure 6(c)) (Matsumura & Komiyama, 1997). Measuring the scission rates over a range of pHs yields a cooperativity coefficient with respect to OH^- close to 1; the curve (Figure 6(d)) closely resembles the analogous one in Figure 3(b) for the inhibition constant, suggesting that indeed backbone scission and inhibition of catalysis are both caused by the same $Tb(OH)(aq)^{2+}$ species (Matsumura & Komiyama, 1997).

These observations suggest a link between the tight terbium(III) binding site in the catalytic core of the hairpin ribozyme, as observed by slow backbone scission, and the potent inhibition of ribozyme catalysis. As plausible this link might be, it should be noted that we cannot completely rule out the existence of other catalytically critical, $Tb(OH)(aq)^{2+}$ binding sites of similarly high affinity that do not lead to backbone scission (Brown *et al.*, 1985). The similarities in affinity, pH dependence, and competition data, however, make the U_{37} scission site a likely candidate for an inhibitory $Tb(OH)(aq)^{2+}$ binding site.

Does scission by $Tb(OH)(aq)^{2+}$ at this site directly lead to inhibition? This possibility seems rather remote, since the observed inhibition occurs instantly after addition of terbium(III) to an active ribozyme-substrate complex and can be reversed (Figure 3(d)), while scission at U_{37} is slow (2 % in two hours; Figure 6(a)) and irreversible. A more likely explanation is that $Tb(OH)(aq)^{2+}$ binds to a site near U_{37} in the 3′-segment of loop B of the ribozyme-substrate complex, changing or restricting the local structure in such a way that the tran-

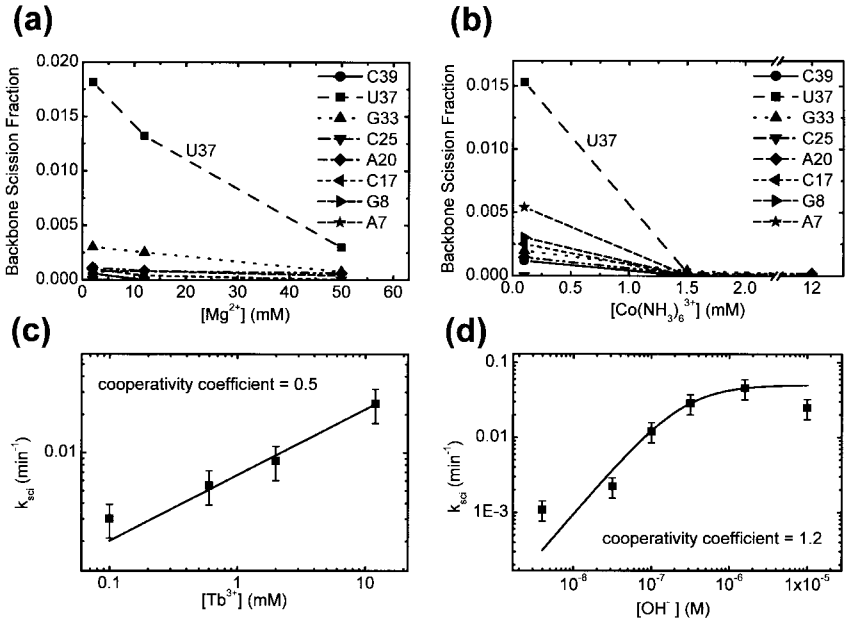

Figure 6. Properties of terbium(III)-mediated footprinting of the hairpin ribozyme at 25 °C. (a) Backbone scission fraction at the eight observed sites in the presence of 100 μM terbium(III), 100 mM Na^+, and increasing concentrations of Mg^{2+} at pH 7.5. (b) Backbone scission fraction at the eight observed sites in the presence of 100 μM terbium(III), 100 mM Na^+, and increasing concentrations of $Co(NH_3)_6^{3+}$ at pH 7.5. (c) Rate constants k_{sci} of backbone scission with increasing terbium(III) concentration in the presence of 100 mM Na^+ and 12 mM Mg^{2+} at pH 7.5. The line represents a fit with the cooperative binding equation (see Materials and Methods), yielding a cooperativity coefficient smaller than 1. (d) Dependence of backbone scission rate constant k_{sci} on hydroxide ion concentration in the presence of 100 mM Na^+ and each 12 mM Mg^{2+} and terbium(III). The line represents a fit with the cooperative binding equation (see Materials and Methods), yielding a cooperativity coefficient close to 1, and an apparent $K_D^{OH^-}$ of $10^{-6.6}$ M (equivalent to a titration midpoint at pH 7.4).

sition state cannot be accessed and inhibition of catalysis is observed, as recently found for the Klenow fragment (Brautigam *et al.*, 1999). Backbone scission then occurs only in a small sub-population of complexes after an extended incubation time, enabling identification of the binding site.

Where in the structure of loop B is this essential terbium(III) binding site? All our experiments were performed on a ribozyme-substrate complex preformed in 200 mM Na^+, before adding a mixture of catalytically proficient cation and terbium(III). Under similar low ionic strength conditions and in the absence of multivalent cations, the NMR solution structure of loop B of the hairpin ribozyme has recently been determined (Butcher *et al.*, 1999). Terbium(III), as other lanthanide(III) metal cations, is known to preferentially bind near one or more negatively charged phosphate oxygens, e.g. in tRNA (Jack *et al.*, 1977; Kim *et al.*, 1985), a notion that is supported by its fast binding kinetics to the hairpin ribozyme (Figure 4(b)). We therefore generated a surface charge plot of the NMR structure of loop B to represent the binding landscape that terbium(III) will encounter in our inhibition experiments. Notably, surface charge plots have yielded surprisingly good indication for metal-ion binding sites in tRNA and the hammerhead ribozyme (Chartrand *et al.*, 1997; Chin *et al.*, 1999).

It is striking that we found an extended area of high negative surface charge potential associated with the 3′-segment of loop B, and created by two sharp kinks in the phosphoribose backbone, due to the bulging of U_{41} (Figure 7(a)). As part of this area and close to U_{37}, a pocket is formed by the three pro-Rp non-bridging oxygens of the phosphates 5′ to A_{38}, C_{39}, and U_{41}, and by N^7 of A_{38} (Figure 7(b)). This pocket is a likely candidate for the metal-ion binding site observed by terbium-mediated inhibition and backbone scission, since: (1) it is close enough to the 2′-hydrogen of U_{37} to deprotonate it in the first step of the observed backbone scission 3′ to U_{37}; (2) it has a large number of potential ligands suitable for terbium(III) binding; (3) it is large enough (spanning 8.55 Å between the phosphate oxygens of A_{38} and U_{41}) to accommodate a hydrated metal ion, which would explain why outer-sphere coordinated cations that promote hairpin ribozyme activity can compete with the inhibitor $Tb(OH)(aq)^{2+}$; and (4) it is located in the major groove of loop B and would remain accessible, as experimentally observed (see above), after the proposed docking of loop A into the minor groove of loop B (Earnshaw *et al.*, 1997; Butcher *et al.*, 1999; Pinard *et al.*, 1999b). The 2′-hydroxyls of A_{24} and C_{25} and the C_{25} base that have been implicated in this docking event of the ribozyme-substrate complex are indicated in Figure 7(b). While docking certainly will have an impact on the local structure of loop B, the NMR structure of the isolated B domain appears to be a

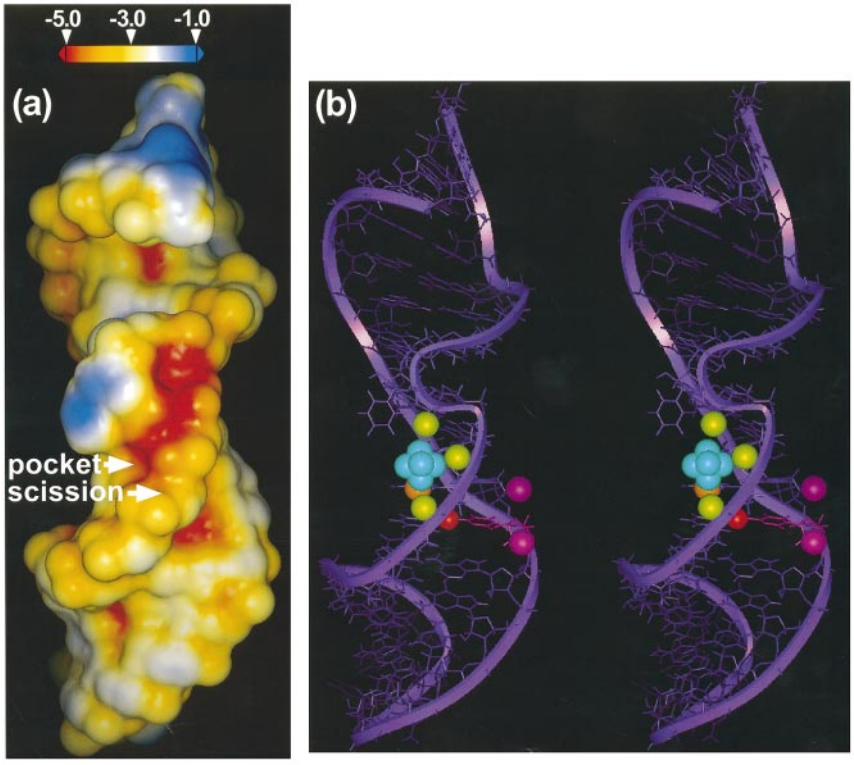

Figure 7. Terbium(III) binds to a region of high negative surface charge potential in loop B of the hairpin ribozyme. (a) Surface charge potential of loop B. Based on the NMR structure (Butcher *et al.*, 1999), the proposed binding pocket for terbium(III) and other cations (see the text) is located in a region of high negative surface charge potential (red). The level of negativity is indicated by the color key. The observed scission site at low concentrations of $Tb(OH)(aq)^{2+}$, 3′ to U_{37}, is indicated. (b) Stereo view of the proposed binding site for a hydrated metal ion in the major groove of the NMR structure of loop B, from the same perspective as (a). Bright blue, hydrated metal ion with inner-sphere water molecules in octahedral coordination; green, pro-R_p non-bridging phosphate oxygen atoms 5′ to A_{38}, C_{39}, and U_{41}, pointing toward the cation binding site; orange, N^7 of A_{38}; red, 2′-hydrogen of U_{37} that becomes removed during backbone scission by terbium(III); bright purple, 2′-oxygen atoms of A_{24} and C_{25} (balls), and C_{25} base, implicated in docking of loop A into the minor groove (located on the right side) of loop B in the ribozyme-substrate complex. Note that docking of loop A is likely not to interfere with the proposed cation binding.

good starting point for discussing some of its structural properties such as potential metal ion binding pockets (Butcher *et al*., 1999).

To test whether the proposed metal ion binding pocket is indeed an outer-sphere coordination site, we asked whether any of the potential RNA ligands close to the observed $Tb(OH)(aq)^{2+}$ binding site are involved in direct coordination of either a Mg^{2+} or a terbium(III) metal ion. To this end, we individually modified the phosphates 5′ to U_{37}, A_{38}, C_{39}, A_{40}, and U_{41} as phosphorothioates (R_P and S_p stereoisomer mixtures) and the N^7 positions of A_{38} and A_{40} as carbons. These modifications substitute soft sulfur for hard oxygen ligands and eliminate soft nitrogen ligands, respectively, so that changes in the relative binding affinities of directly coordinated hard Mg^{2+} *versus* soft terbium(III) metal ions would be expected (Feig & Uhlenbeck, 1999). However, we did not observe changes in the terbium(III) inhibition constants in the presence of 12 mM Mg^{2+} for any of these modifications (data not shown), consistent with a model in which a terbium(III) bound in the proposed binding pocket is not directly coordinated to the RNA. The observed terbium(III) binding site, therefore, appears to be a catalytically essential, but rather non-selective outer-sphere cation binding site, offering a plausible explanation for the lack in cation cofactor selectivity of the hairpin ribozyme.

Discussion

$Tb(OH)(aq)^{2+}$ interferes with a late step in hairpin ribozyme catalysis

The hairpin ribozyme can cleave its substrate RNA under a variety of cationic conditions that include monovalent cations, soft and hard divalent cations, kinetically non-exchangeable complexes of trivalent metal ions, e.g. cobalt(III) hexammine, and organic polyamines (Walter & Burke, 1998; Murray *et al*., 1998; Earnshaw & Gait, 1998; Nesbitt *et al*., 1999). In fact, only a few cations appear to be incompatible with catalytic activity, as long as they are used in an appropriate concentration range. We now have characterized such an inhibitory aqueous metal ion complex, $Tb(OH)(aq)^{2+}$. Inhibition appears to be sensitive to the overall charge of the terbium(III) complex, as protonation reverses inhibition. At pH values significantly below the pK_a of terbium(III) (7.9), a bell-shaped dependence of hairpin ribozyme activity on the total lanthanide(III) ion concentration is observed. An analogous effect is seen in the presence of lanthanum(III) as the inhibitory cation ($pK_a(La^{3+}) = 8.5$). These metal ion dependencies resemble that of the hammerhead ribozyme on lanthanum(III) at a pH of 7.0, which was interpreted as evidence for a two-metal ion mechanism (Lott *et al*., 1998). It is important to keep in mind that not only two distinct metal-ion binding sites, but also the presence of two different aqueous lanthanide(III) ion complexes in solution, such as $Ln(aq)^{3+}$ and $Ln(OH)(aq)^{2+}$, can lead to a bell-shaped activation curve, as shown here for the hairpin ribozyme.

Higher (millimolar) concentrations of terbium(III) interfere with both formation and docking of the ribozyme-substrate complex, as shown by terbium(III)-mediated backbone scission (Figure 5(a)). However, we were also able to demonstrate, by fluorescence resonance energy transfer (Figure 4(e)) and hydroxyl radical footprinting, that lower terbium(III) concentrations (micromolar) do not interfere with domain docking of the complex, yet still inhibit cleavage activity. Hence, inhibition at micromolar terbium(III) concentration can be attributed to blockage of a post-docking step in the reaction pathway (Figure 1(b)).

How does $Tb(OH)(aq)^{2+}$ inhibit hairpin ribozyme activity? Inhibition occurs instantly and is reversible, as was shown previously for the hammerhead ribozyme (Feig *et al*., 1998), ruling out slow and irreversible chemical damage to the RNA as mode of interference. The rate-limiting step of hairpin ribozyme-catalyzed cleavage occurs after global docking of the ribozyme-substrate complex (Walter *et al*., 1998; Hampel *et al*., 1998) and is pH-independent (Nesbitt *et al*., 1997), consistent with the notion that a localized conformational change might be the slowest step in the cleavage reaction pathway. In impairing cleavage, a proximal $Tb(OH)(aq)^{2+}$ might alter the geometry of the sugar-phosphate backbone and the base-stacking interactions required for this conformational change, or a tightly bound $Tb(OH)(aq)^{2+}$ might constrain the flexibility of the complex (Gersanovski *et al*., 1985; Tajmir-Riahi *et al*., 1993; Brautigam *et al*., 1999), to a degree that is incompatible with catalytic activity. The possibility that terbium interferes with the as yet undefined rate-limiting step in hairpin ribozyme catalysis makes it a useful probe to further characterize the reaction mechanism of this and potentially other RNA catalysts.

Terbium(III) is a versatile probe of RNA structure, function, and metal-ion binding

We found that backbone scission with 12 mM terbium(III) at pH 7.5, after a two-hour incubation at room temperature, produces a distinct footprinting pattern of hairpin ribozyme secondary and tertiary structure, analogous to hydroxyl radical footprinting (Hampel *et al*., 1998). Terbium(III) concentrations down to 2 mM, any pH above 7.0, or shorter incubation times ($\geqslant$30 minutes) yield similar patterns (data not shown). Unlike hydroxyl radicals, terbium(III) ions preferentially cut non-Watson-Crick base-paired regions, making them a powerful and easy-to-use probe for the solvent accessibility of structural elements in RNA that typically are involved in long-range tertiary contacts or protein binding. Interestingly, terbium(III) at these high concentrations can interfere with the formation of both secondary and tertiary structure,

but it does not disrupt pre-formed structures, so that RNA folding pathways can be revealed by order-of-addition experiments. These applications expand the previously described use of lanthanide(III)-mediated backbone cleavage in detection of specific metal-ion binding sites in RNA (Ciesiolka *et al*., 1989; Evans, 1990; Gast *et al*., 1996; Feig & Uhlenbeck, 1999), or in RNA degradation for biotechnological applications (Stein & Cohen, 1988; Morrow, 1996; Matsumura & Komiyama, 1997). Our results are also distinct from backbone scission by other metal ions such as lead, that typically display a much narrower range of scission sites (Ciesiolka *et al*., 1989).

Why does terbium(III) scission preferentially cleave the backbone of non-Watson-Crick base-paired regions in RNA? The interaction of terbium(III) ions with nucleic acids occurs both with the negatively charged phosphate oxygens of the backbone and the electron donor groups on the nucleoside bases, in particular the N^7 position of purines (Gross & Simpkins, 1981; Gersanovski *et al*., 1985; Tajmir-Riahi *et al*., 1993; Feig *et al*., 1998) and possibly the base Π-electron systems (McFail-Isom *et al*., 1998). It is well conceivable that the better accessibility of these groups in the widened major groove of non-Watson-Crick base-paired regions in RNA stabilizes binding of terbium to these segments and, as a result, leads to a higher probability of backbone scission. The affinity of the hairpin ribozyme for the most tightly binding terbium(III) ions is about three orders of magnitude higher than the one for magnesium(II), as observed in our competition experiments. Hence, the high binding free energy of terbium(III) may stabilize unstacked conformations of weakly (non-Watson-Crick) base-paired nucleoside bases, which might explain the observed inhibition of ribozyme activity (Feig *et al*., 1998; and results presented herein).

Terbium(III), like other lanthanide metal ions, particularly europium(III), permits fluorescence analysis of its binding sites on nucleic acids by energy transfer from guanine bases (Yonushot *et al*., 1978; Topal & Fresco, 1980; Wenzel & Collette, 1988). We have used this effect to distinguish classes of binding sites with different affinities as well as distinct processes in the binding kinetics of terbium(III) to the hairpin ribozyme. In addition, using more sophisticated spectroscopic equipment, the detailed fluorescence properties of nucleic acid-bound terbium(III) or europium(III) ions can yield information on the number and nature of their inner-sphere ligands (Horrocks, 1993; Feig *et al*., 1999). Taken together, these properties make lanthanide(III) ions versatile probes for the analysis of structure, function, and metal-ion binding sites in RNA.

Terbium(III) reveals an outer-sphere metal-ion binding site

RNA backbone scission at micromolar terbium(III) concentrations was used to identify a high-affinity terbium(III) binding site of the hairpin ribozyme in an area of loop B with high negative surface charge potential. Both terbium(III) binding to this site and inhibition of catalytic activity share similar affinities and can be competed by any cation known to promote hairpin ribozyme activity. The involved functionally important binding pocket(s), therefore, must be able to accommodate a wide variety of cations, including Mg^{2+}, Mn^{2+}, $Co(NH_3)_6^{3+}$, spd^{+++}, and Na^+. Although we cannot completely rule out inner-sphere coordination of some of these cations, the observations that cobalt(III) hexammine and polyamines bind despite their inability to coordinate RNA ligands and that Tb^{3+} binding is not influenced by RNA modifications designed to interfere with directly coordinated metal ions suggest that inner-sphere coordination is not a requirement for binding to this site. Thus, the proposed binding pocket in the major groove of loop B appears to be a member of the third class of the metal-ion binding sites as described by Laing *et al*. (1994); binding occurs site-specifically, but non-selectively in an area of RNA with unusually high charge density. Because of its variability and solvent accessibility, this type of cation-binding site can be expected to be difficult to identify by structure determination methods such as NMR and X-ray crystallography.

A cation site-specifically bound in an area of high negative surface charge potential can be expected to substantially contribute to the stability of RNA tertiary structure contacts close to this area. In the case of the hairpin ribozyme, the proposed cation binding pocket maps proximal to the proposed tertiary contacts between loops A and B (Figure 7(b)) (Earnshaw *et al*., 1997; Butcher *et al*., 1999; Pinard *et al*., 1999b) and stays occupied before and after tertiary structure folding. Our competition data suggest that it is indeed the site typically detected by metal-ion titration of cleavage activity (Nesbitt *et al*., 1997, 1999; Walter *et al*., 1998; Thomson & Lilley, 1999). By contrast, many additional metal ions are more weakly bound to the loop regions of the undocked conformation and become displaced upon tertiary structure formation, as observed by terbium(III)-mediated footprinting. Hence, despite its lack in inner-sphere contacts, the proposed cation binding pocket shares some features with the classic ''specific'' metal-ion binding sites that are observed in the tertiary structure of large RNA catalysts (Celander & Cech, 1991; Smith *et al*., 1992; Cate & Doudna, 1996; Cate *et al*., 1996, 1997; Basu *et al*., 1998).

The unusually high negative charge density of the proposed cation binding pocket is created by two subsequent kinks in the backbone of the hairpin ribozyme, due to two extra nucleotides in the 3′-segment of loop B (Figure 7) (Butcher *et al*., 1999). Interestingly, the associated motif has been found to also organize the structure of multi-helix loops in 16 S and 23 S ribosomal RNA (Leontis & Westhof, 1998), two of the most ancient RNAs, extensively used for phylogenetic classification of

the ''tree of life'' (Doolittle, 1999). Other structural elements in RNA that are able to bind outer-sphere coordinated metal ions in their major groove are G:U wobble or G:A sheared base-pairs, or GNRA tetraloops (Cate & Doudna, 1996; Kieft & Tinoco, 1997; Suga *et al*., 1998; Wedekind & McKay, 1998; Feig & Uhlenbeck, 1999). These elements also have been identified as building blocks for the more complex binding sites of specific metal ions in larger RNAs (Cate *et al*., 1996, 1997). It is therefore tempting to propose that outer-sphere metal-ion binding sites emerged first in the primitive ribozymes of the early RNA world, ultimately becoming buried in the complex tertiary structures of the subsequently evolving larger RNA catalysts. Notably, even in these structures metal ions remain significantly hydrated (Feig & Uhlenbeck, 1999). We now have identified such an outer-sphere metal-ion binding element in the hairpin ribozyme and have related it to the function of this RNA catalyst.

Materials and Methods

Synthesis and purification of oligonucleotides

RNA oligonucleotides were synthesized by standard methods using solid-phase phosphoramidite chemistry from Glen Research implemented on an Applied Biosystems 392 DNA/RNA synthesizer (1 μmol scale). 3′-Fluorescein and 5′-hexachlorofluorescein for FRET analysis were attached during synthesis as described (Walter *et al*., 1998), oxidation with S_8 was used to generate a stereoisomer (R_P and S_P) mixture of site-specific phosphorothioates, and the N7-deaza-ribo adenosine phosphoramidite was purchased from ChemGenes. Synthetic RNA was deprotected following the protocol of Wincott *et al*. (1995), utilizing a 3:1 mixture of concentrated aqueous ammonia and ethanol to remove the exocyclic amine protection groups and triethylamine trihydrofluoride to remove the 2′ OH silyl protection groups. Fully deprotected, full-length RNA was isolated by denaturing, 8 M urea, 20 % (w/v) polyacrylamide gel electrophoresis, diffusion elution from the gel slices, ethanol precipitation, and subsequent C_8-reversed phase HPLC with a gradient of 0-60 % acetonitrile in 0.1 M triethyl ammonium acetate (50 minutes, 1 ml/minute). Non-cleavable, chemically blocked substrate analog was obtained by introducing a deoxy-A (dA) modification at the cleavage site (position −1).

The ribozyme was transcribed from two synthetic, fully complementary and annealed DNA strands, basically as described (Milligan & Uhlenbeck, 1989), except that higher NTP concentrations (7.5 mM each) together with inorganic pyrophosphatase were used to increase yields (Cunningham & Ofengand, 1990). The full-length run-off transcript was isolated after denaturing, 8 M urea, 10 % (w/v) polyacrylamide gel electrophoresis by UV shadowing, diffusion elution of the gel slices, and ethanol precipitation.

Handling of cation stock solutions

For all salts, the highest available purity from Sigma or Aldrich was used, with chloride as the common anionic component. Stock solutions of Tb^{3+}, Mn^{2+}, and $Co(NH_3)_6^{3+}$ were kept in small aliquots at −20 °C in the dark to avoid oxidation or precipitation. $TbCl_3$ was dissolved to 1 mM, 10 mM, or 100 mM in a 5 mM sodium cacodylate buffer at pH 5.5 to prevent formation of terbium(III) hydroxide precipitates at higher pH. Spermidine and spermine stock solutions (1 M and 100 mM, respectively) were brought to pH 7.5 by titrating the dissolved hydrochloride salts with NaOH.

Radioactive cleavage reactions

(5′-^{32}P)-labeled substrate was prepared by phosphorylation with T4 polynucleotide kinase and [γ-^{32}P]ATP, and was purified using CentriSep spin columns (Princeton Separations). Trace amounts (<1 nM) of radiolabeled substrate and 200 nM transcribed hairpin ribozyme (Figure 1(a)) were annealed in the absence of multivalent cations (in 100 mM Tris-HCl (pH 7.5), 200 mM NaCl; note that the subsequent addition of an equal volume of cation stock solution (see below) lowered these concentrations to 50 mM and 100 mM, respectively) at 25 °C for 15 minutes. To obtain other pH values, the following buffers were used instead of Tris-HCl; MES-NaOH for pH 5.6 and 6.5; Pipes-NaOH for pH 7.0; TAPS-NaOH, for pH 8.2 and 9.0. To initiate cleavage, an equal volume of cation stock solution (containing only the cations required to give the final concentrations as described in Results) at 25 °C was added. Typically ten 5-μl aliquots of the reaction were taken over a two-hour period and stopped by mixing with at least an equal volume of ice-chilled loading buffer (80 % (v/v) formamide, 0.025 % (w/v) xylene cyanol, 0.025 % (w/v) bromophenol blue, 50 mM EDTA). The 5′ cleavage product was separated from uncleaved substrate by denaturing, 8 M urea, 20 % polyacrylamide gel electrophoresis, quantified, and normalized to the sum of the substrate and product bands using a Bio-Rad Molecular Imager System GS-525. The time trace of product formation was fitted to the exponential growth equation $y = y_0 + A_1(1 - e^{-t/\tau 1}) + A_2(1 - e^{-t/\tau 2})$, as described by Esteban *et al*. (1997). The data sets in the presence of terbium(III) were fitted satisfactorily with single-exponentials ($A_1 \neq 0$, $A_2 = 0$), while other data sets, notably those in the presence of Mg^{2+} and $Co(NH_3)_6^{3+}$, required double-exponentials (A_1, $A_2 \neq 0$), as described by Esteban *et al*. (1997); in addition, the presence of terbium(III) often lowered the amplitudes rather than the rate constants. Therefore, a rate constant k was calculated from $k = A_1/t_1 + A_2/t_2$ to account for the influence of terbium(III) on cleavage rate and fraction of the two phases of hairpin ribozyme cleavage. Ratios of the obtained rate constants were plotted over different cation concentrations to analyze the data using the cooperative-binding equation:

$$y = y_{\max} \frac{[M^{n+}]^p}{[M^{n+}]^p + K_D^p}$$

yielding an apparent dissociation constant K_D^M for cation M^{n+} (or the corresponding apparent inhibition constant K_i for Tb^{3+}) and a cooperativity or Hill coefficient p. All fits were calculated using Microcal™ Origin™ 4.1 software employing Marquardt-Levenberg non-linear least-squares regression.

Steady-state fluorescence measurements

Steady-state fluorescence intensities of a doubly fluorophore-labeled two-piece hairpin ribozyme were recorded on an Aminco-Bowman Series 2 (AB2) spectro-

fluorometer from SLM (Rochester, NY) in a cuvette with 3-mm excitation and emission path lengths (150 µl total volume), essentially as described (Walter *et al*., 1998). 200 nM ribozyme-substrate complex were constituted in 50 mM Tris-HCl (pH 7.5), 100 mM NaCl, 25 mM DTT (final concentration), by addition of each 500 nM non-cleavable (dA_{-1}) substrate analog and unlabeled ribozyme 3′-segment to 200 nM of the 5′-hexachlorofluorescein and 3′-fluorescein doubly-labeled ribozyme 5′-segment, heating to 70 °C for two minutes, and cooling to room temperature over five minutes. The obtained complex was pre-incubated at 25 °C for 15 minutes, before manually mixing 145 µl complex solution with 5 µl cation stock solution in the fluorometer cuvette to give final concentrations of 12 mM $MgCl_2$ and up to 100 µM Tb^{3+}. Tertiary structure formation was monitored as steady-state fluorescence changes of the two fluorophores over time. Fluorescein was excited at 485 nm (4 nm slit width), and fluorescence emission was monitored both at 515 nm and 545 nm (8 nm slit width) by shifting the emission monochromator back and forth, using the AB2 software package, and a ratio $Q = F_{545}/F_{515}$ reflecting the FRET efficiency was calculated. Q was normalized with its value Q_0 immediately after formation of the substrate-ribozyme complex (i.e. $(Q - Q_0)/Q_0$ was calculated). The resulting growth curves were fitted to the single-exponential function $y = y_0 + A(1 - e^{-t/\tau})$ to yield the docking rate constant $k_{dock} = 1/\tau$ and the docking amplitude A.

Steady-state fluorescence spectra of Tb^{3+} bound to 1 µM of the pre-formed complex of ribozyme (Figure 1(a)) with non-cleavable (dA_{-1}) substrate analog were measured in standard reaction buffer (50 mM Tris-HCl (pH 7.5), 12 mM $MgCl_2$) at 25 °C, by slowly titrating $TbCl_3$ over several orders of magnitude from appropriate stock solutions. Excitation was at 290 nm (slit width 4 nm), steady-state emission was scanned with a slit width of 8 nm. To extract the fluorescence intensity of the major peak at 545 nm, each peak was fitted between 530 nm and 555 nm with the Gaussian distribution function:

$$y = y_0 + \frac{A}{w\sqrt{\pi/2}} e^{-2\frac{(x-x_0)^2}{w^2}}$$

to yield the peak height as the pre-exponential factor, from which the background value in the absence of Tb^{3+} was subtracted. These fluorescence signals were plotted over varying Tb^{3+} concentration and were fitted with Hill equations as described above. For a fit over the complete Tb^{3+} titration range, a sum of three independent Hill equations produced the best result.

Stopped-flow kinetic experiments were performed using the Milli-Flow Reactor from SLM (Rochester, NY) on the AB2 spectrofluorometer. A stock solution of 4 mM Tb^{3+} in standard reaction buffer (50 mM Tris-HCl (pH 7.5), 12 mM $MgCl_2$) was mixed with an equal volume of the same buffer, with or without 2 µM pre-formed complex of ribozyme (Figure 1(a)) with non-cleavable (dA_{-1}) substrate analog at 25 °C. Excitation was at 290 nm (slit width 8 nm), emission was at 545 nm (slit width 8 nm), and changes in steady-state fluorescence intensity were recorded for ten seconds in 1 ms time intervals. In the presence of the ribozyme-substrate complex, a fluorescence increase was observed that could only be fitted satisfactorily with a growth equation with at least three exponentials, $y = y_0 + A_1(1 - e^{-t/\tau 1}) + A_2(1 - e^{-t/\tau 2}) + A_3(1 - e^{-t/\tau 3})$. Rate constants were calculated from $k = 1/\tau$.

Terbium(III)-mediated footprinting

To observe the slow backbone scission reaction mediated by $Tb(OH)(aq)^{2+}$, transcribed ribozyme (Figure 1(a)) was dephosphorylated with an excess of calf intestine alkaline phosphatase for one hour at 37 °C, phenol/chloroform extracted, recovered by ethanol precipitation, (5′-^{32}P)-phosphorylated using T4 polynucleotide kinase and [γ-^{32}P]ATP, desalted using a CentriSep spin column (Princeton Separations), and purified by denaturing, 8 M urea, 10 % polyacrylamide gel electrophoresis, followed by diffusion elution into 5 mM EDTA, ethanol precipitation in the presence of 1 mM ATP as carrier, and desalting using a CentriSep spin column. The labeled ribozyme (typically ~500,000 dpm per 10-µl reaction, or ~5 nM) was incubated with varying additives in the presence of typically 12 mM $TbCl_3$ for two hours at 25 °C. To fold the tertiary structure of the ribozyme-substrate complex, Mg^{2+} or cobalt(III) hexammine had to be added five minutes prior to terbium(III). The scission reaction was stopped by addition of an equal volume of 80 % formamide, 50 mM EDTA, and analyzed on an 8 M urea, 15 % wedged polyacrylamide sequencing gel, alongside sequencing ladders from partial digestion with ribonucleases T_1 and U_2, and alkali hydrolysis (Pinard *et al*., 1999a). For time courses, typically eight aliquots were taken over three to six hours. Product bands were either visualized using autoradiography or quantified and normalized to the sum of the substrate and product bands (after subtraction of background degradation in the absence of terbium(III)) using a Bio-Rad Molecular Imager System GS-525; scission rate constants k_{sci} were calculated from a fit $y = y_0 + A(1 - e^{-t/\tau})$ to the combined scission fractions at all cut positions, with $k_{sci} = 1/\tau$.

Molecular modeling

The NMR structure of loop B of the hairpin ribozyme as deposited in the RCSB Protein Data Bank, accession number 1B36 (Butcher *et al*., 1999) with a bound hydrated metal ion was visualized using the program Insight II (MSI/Biosym). Electrostatic potentials were calculated using the finite difference non-linear Poisson-Boltzmann equation implemented in the program Delphi (Molecular Simulations Inc., San Diego 1995) and mapped, using Insight II, onto the molecular surface of loop B, created by rolling a spherical probe corresponding to the radius of a water molecule (1.4 Å) around the exterior. The Amber-like partial charges for RNA were taken from Tung *et al*. (1984).

Acknowledgments

We are grateful to David Pecchia for RNA synthesis, to Krishnan Venkataraman, Ken Hampel, and Erika Albinson for contribution of experimental data and helpful discussions, and to Jeffrey Bond and his Molecular Modeling Facility of the Vermont Cancer Center for help with Figure 7.

References

Baes, C. F. & Mesmer, R. E. (1976). *The Hydrolysis of Cations*, pp. 129-146, Wiley-Interscience, New York.

Basu, S., Rambo, R. P., Strauss-Soukup, J., Cate, J. H., Ferré-D'Amaré, A. R., Strobel, S. A. & Doudna, J. A. (1998). A specific monovalent metal ion integral to the AA platform of the RNA tetraloop receptor. *Nature Struct. Biol.* **5**, 986-992.

Been, M. D. & Wickham, G. S. (1997). Self-cleaving ribozymes of hepatitis delta virus RNA. *Eur. J. Biochem.* **247**, 741-753.

Brautigam, C. A., Aschheim, K. & Steitz, T. A. (1999). Structural elucidation of the binding and inhibitory properties of lanthanide (III) ions at the 3′-5′ exonucleolytic active site of the Klenow fragment. *Chem. Biol.* **6**, 901-908.

Brown, R. S., Dewan, J. C. & Klug, A. (1985). Crystallographic and biochemical investigation of the lead(II)-catalyzed hydrolysis of yeast phenylalanine tRNA. *Biochemistry,* **24**, 4785-4801.

Butcher, S. E., Allain, F. H. T. & Feigon, J. (1999). Solution structure of the loop B domain from the hairpin ribozyme. *Nature Struct. Biol.* **6**, 212-216.

Buzayan, J. M., Gerlach, W. L. & Bruening, G. (1986). Non-enzymatic cleavage and ligation of RNAs complementary to a plant virus satellite RNA. *Nature,* **323**, 349-353.

Cai, Z. & Tinoco, I. (1996). Solution structure of loop A from the hairpin ribozyme from tobacco ringspot virus satellite. *Biochemistry,* **35**, 6026-6036.

Cate, J. H. & Doudna, J. A. (1996). Metal-binding sites in the major groove of a large ribozyme domain. *Structure,* **4**, 1221-1229.

Cate, J. H., Gooding, A. R., Podell, E., Zhou, K., Golden, B. L., Kundrot, C. E., Cech, T. R. & Doudna, J. A. (1996). Crystal structure of a group I ribozyme domain: principles of RNA packing. *Science,* **273**, 1678-1685.

Cate, J. H., Hanna, R. L. & Doudna, J. A. (1997). A magnesium ion core at the heart of a ribozyme domain. *Nature Struct. Biol.* **4**, 553-558.

Cech, T. (1993). Structure and Mechanism of the large catalytic RNAs: group I and group II introns and ribonuclease P. In *RNA World* (Gesteland, R. F. & Atkins, J. F., eds), pp. 239-269, Cold Spring Harbor Laboratory Press, Cold Spring Harbor, NY.

Celander, D. W. & Cech, T. R. (1991). Visualizing the higher order folding of a catalytic RNA molecule. *Science,* **251**, 401-407.

Chartrand, P., Leclerc, F. & Cedergren, R. (1997). Relating conformation, Mg^{2+} binding, and functional group modification in the hammerhead ribozyme. *RNA,* **3**, 692-696.

Chin, K., Sharp, K. A., Honig, B. & Pyle, A. M. (1999). Calculating the electrostatic properties of RNA provides new insights into molecular interactions and function. *Nature Struct. Biol.* **6**, 1055-1061.

Ciesiolka, J., Marciniec, T. & Krzyzosiak, W. (1989). Probing the environment of lanthanide binding sites in yeast $tRNA^{Phe}$ by specific metal-ion-promoted cleavages. *Eur. J. Biochem.* **182**, 445-450.

Cunningham, P. R. & Ofengand, J. (1990). Use of inorganic pyrophosphatase to improve the yield of *in vitro* transcription reactions catalyzed by T7 RNA polymerase. *Biotechniques,* **9**, 713-714.

Dickeson, S. K., Bhattacharyya-Pakrasi, M., Mathis, N. L., Schlesinger, P. H. & Santoro, S. A. (1998). Ligand binding results in divalent cation displacement from the α2β1 integrin I domain: evidence from terbium luminescence spectroscopy. *Biochemistry,* **37**, 11280-11288.

Doolittle, W. F. (1999). Phylogenetic classification and the universal tree. *Science,* **284**, 2124-2129.

Draper, D. E. (1985). On the coordination properties of Eu^{3+} bound to tRNA. *Biophys. Chem.* **21**, 91-101.

Earnshaw, D. J. & Gait, M. J. (1997). Progress toward the structure and therapeutic use of the hairpin ribozyme. *Antisense Nucleic Drug Dev.* **7**, 403-411.

Earnshaw, D. J. & Gait, M. J. (1998). Hairpin ribozyme cleavage catalyzed by aminoglycoside antibiotics and the polyamine spermine in the absence of metal ions. *Nucl. Acids Res.* **26**, 5551-5561.

Earnshaw, D. J., Masquida, B., Müller, S., Sigurdsson, S. T., Eckstein, F., Westhof, E. & Gait, M. J. (1997). Inter-domain cross-linking and molecular modelling of the hairpin ribozyme. *J. Mol. Biol.* **247**, 1-16.

Esteban, J. A., Banerjee, A. R. & Burke, J. M. (1997). Kinetic mechanism of the hairpin ribozyme. Identification and characterization of two nonexchangeable conformations. *J. Biol. Chem.* **272**, 13629-13639.

Evans, C. H. (1990). *The Biochemistry of Lanthanides*, pp. 85-204, Plenum Press, London.

Faulhammer, D. & Famulok, M. (1997). Characterization and divalent metal-ion dependence of *in vitro* selected deoxyribozymes which cleave DNA/RNA chimeric oligonucleotides. *J. Mol. Biol.* **269**, 188-202.

Feig, A. L. & Uhlenbeck, O. C. (1999). The role of metal ions in RNA biochemistry. In *RNA World* (Gesteland, R. F., Cech, T. R. & Atkins, J. F., eds), 2nd edit., pp. 287-319, Cold Spring Harbor Laboratory Press, Cold Spring Harbor, NY.

Feig, A. L., Scott, W. G. & Uhlenbeck, O. C. (1998). Inhibition of the hammerhead ribozyme cleavage reaction by site-specific binding of Tb. *Science,* **279**, 81-84.

Feig, A. L., Panek, M., Horrocks, W. D. & Uhlenbeck, O. C. (1999). Probing the binding of Tb(III) and Eu(III) to the hammerhead ribozyme using luminescence spectroscopy. *Chem. Biol.* **6**, 801-810.

Frey, M. W., Frey, S. T., Horrocks, W. D., Kaboord, B. F. & Benkovic, S. J. (1996). Elucidation of the metal-binding properties of the Klenow fragment of *Escherichia coli* polymerase I and bacteriophage T4 DNA polymerase by lanthanide(III) luminescence spectroscopy. *Chem. Biol.* **3**, 393-403.

Gast, F. U., Kempe, D., Spieker, R. L. & Sanger, H. L. (1996). Secondary structure probing of potato spindle tuber viroid (PSTVd) and sequence comparison with other small pathogenic RNA replicons provides evidence for central non-canonical base-pairs, large A-rich loops, and a terminal branch. *J. Mol. Biol.* **262**, 652-670.

Gersanovski, D., Colson, P., Houssier, C. & Fredericq, E. (1985). Terbium(3+) as a probe of nucleic acids structure. Does it alter the DNA conformation in solution?. *Biochim. Biophys. Acta,* **824**, 313-323.

Geyer, C. R. & Sen, D. (1997). Evidence for the metal-cofactor independence of an RNA phosphodiester-cleaving DNA enzyme. *Chem. Biol.* **4**, 579-593.

Gross, D. S. & Simpkins, H. J. (1981). Evidence for two-site binding in the terbium(III)-nucleic acid interaction. *J. Biol. Chem.* **256**, 9593-9598.

Hampel, A. & Cowan, J. A. (1997). A unique mechanism for RNA catalysis: the role of metal cofactors in hairpin ribozyme cleavage. *Chem. Biol.* **4**, 513-517.

Hampel, A. & Tritz, R. (1989). RNA catalytic properties of the minimum (−)sTRSV sequence. *Biochemistry,* **28**, 4929-4933.

Hampel, K. J., Walter, N. G. & Burke, J. M. (1998). The solvent-protected core of the hairpin ribozyme-substrate complex. *Biochemistry,* **37**, 14672-14682.

Horrocks, W. D. (1993). Luminescence spectroscopy. *Methods Enzymol.* **226**, 495-538.

Horrocks, W. D., Schmidt, G. F., Sudnick, D. R., Kittrell, C. & Bernheim, R. A. (1977). Laser-induced lanthanide ion luminescence lifetime measurements by direct excitation of metal ion levels. A new class of structural probe for calcium-binding proteins and nucleic acids. *J. Am. Chem. Soc.* **99**, 2378-2380.

Jack, A., Ladner, J. E., Rhodes, D., Brown, R. S. & Klug, A. (1977). A crystallographic study of metal-binding to yeast phenylalanine transfer RNA. *J. Mol. Biol.* **111**, 315-328.

Jayasena, V. K. & Gold, L. (1997). *In vitro* selection of self-cleaving RNAs with a low pH optimum. *Proc. Natl Acad. Sci. USA,* **94**, 10612-10617.

Kieft, J. S. & Tinoco, I. (1997). Solution structure of a metal-binding site in the major groove of RNA complexed with cobalt(III) hexammine. *Structure,* **5**, 713-721.

Kim, S. H., Shin, W. C. & Warrant, R. W. (1985). Heavy metal ion-nucleic acid interaction. *Methods Enzymol.* **114**, 156-167.

Laing, L. G., Gluick, T. C. & Draper, D. E. (1994). Stabilization of RNA structure by Mg ions. Specific and non-specific effects. *J. Mol. Biol.* **237**, 577-587.

Leontis, N. B. & Westhof, E. (1998). A common motif organizes the structure of multi-helix loops in 16 S and 23 S ribosomal RNAs. *J. Mol. Biol.* **283**, 571-583.

Lott, W. B., Pontius, B. W. & von Hippel, P. H. (1998). A two-metal ion mechanism operates in the hammerhead ribozyme-mediated cleavage of an RNA substrate. *Proc. Natl Acad. Sci. USA,* **95**, 542-547.

Matsumura, K. & Komiyama, M. (1997). Enormously fast hydrolysis by lanthanide(III) ions under physiological conditions: eminent candidates for novel tools of biotechnology. *J. Biochem.* **122**, 387-394.

McFail-Isom, L., Shui, X. & Williams, L. D. (1998). Divalent cations stabilize unstacked conformations of DNA and RNA by interacting with base π systems. *Biochemistry,* **37**, 17105-17111.

Milligan, J. F. & Uhlenbeck, O. C. (1989). Synthesis of small RNAs using T7 RNA polymerase. *Methods Enzymol.* **180**, 51-62.

Morrow, J. R. (1996). Hydrolytic cleavage of RNA catalyzed by metal ion complexes. *Methods Ions Biol. Syst.* **33**, 561-592.

Murchie, A. I., Thomson, J. B., Walter, F. & Lilley, D. M. (1998). Folding of the hairpin ribozyme in its natural conformation achieves close physical proximity of the loops. *Mol. Cell,* **1**, 873-881.

Murray, J. B., Seyhan, A. A., Walter, N. G., Burke, J. M. & Scott, W. G. (1998). The hammerhead, hairpin and VS ribozymes are catalytically proficient in monovalent cations alone. *Chem. Biol.* **5**, 587-595.

Narlikar, G. J. & Herschlag, D. (1997). Mechanistic aspects of enzymatic catalysis: lessons from comparison of RNA and protein enzymes. *Annu. Rev. Biochem.* **66**, 19-59.

Nesbitt, S., Hegg, L. A. & Fedor, M. J. (1997). An unusual pH-independent and metal-ion-independent mechanism for hairpin ribozyme catalysis. *Chem. Biol.* **4**, 619-630.

Nesbitt, S. M., Erlacher, H. A. & Fedor, M. J. (1999). The internal equilibrium of the hairpin ribozyme: temperature, ion and pH effects. *J. Mol. Biol.* **286**, 1009-1024.

Pan, T. & Uhlenbeck, O. C. (1992). A small metalloribozyme with a two-step mechanism. *Nature,* **358**, 560-563.

Pan, T., Long, D. M. & Uhlenbeck, O. C. (1993). Divalent metal ions in RNA folding and catalysis. In *RNA World* (Gesteland, R. F., Cech, T. R. & Atkins, J. F., eds), pp. 271-302, Cold Spring Harbor Laboratory Press, Cold Spring Harbor, NY.

Pinard, R., Heckman, J. E. & Burke, J. M. (1999a). Alignment of the two domains of the hairpin ribozyme-substrate complex defined by interdomain photoaffinity crosslinking. *J. Mol. Biol.* **287**, 239-251.

Pinard, R., Lambert, D., Walter, N. G., Heckman, J. E., Major, F. & Burke, J. M. (1999b). Structural basis for the guanosine requirement of the hairpin ribozyme. *Biochemistry,* **38**, 16035-16039.

Pyle, A. M. (1993). Ribozymes: a distinct class of metalloenzymes. *Science,* **261**, 709-714.

Pyle, A. M. (1996). Role of metal ions in ribozymes. *Metal Ions Biol. Syst.* **32**, 479-520.

Sigurdsson, S. T., Thomson, J. B. & Eckstein, F. (1998). Small ribozymes. In *RNA Structure and Function* (Simons, R. W. & Grunberg-Manago, M., eds), pp. 339-375, Cold Spring Harbor Press, Cold Spring Harbor, NY.

Smith, D. (1995). Magnesium as the catalytic center of RNA enzymes. In *The Biological Chemistry of Magnesium* (Cowan, J. A., ed.), pp. 111-136, VCH, New York.

Smith, D., Burgin, A. B., Haas, E. S. & Pace, N. R. (1992). Influence of metal ions on the ribonuclease P reaction. Distinguishing substrate binding from catalysis. *J. Biol. Chem.* **267**, 2429-2436.

Stein, C. A. & Cohen, J. A. (1988). Oligodeoxynucleotides as inhibitors of gene expression: a review. *Cancer Res.* **48**, 2659-2668.

Steitz, T. A. & Steitz, J. A. (1993). A general two-metal-ion mechanism for catalytic RNA. *Proc. Natl Acad. Sci. USA,* **90**, 6498-6502.

Suga, H., Cowan, J. A. & Szostak, J. W. (1998). Unusual metal ion catalysis in an acyl-transferase ribozyme. *Biochemistry,* **37**, 10118-10125.

Tajmir-Riahi, H. A., Ahmad, R. & Naoui, M. J. (1993). Interaction of calf-thymus DNA with trivalent La, Eu, and Tb ions. Metal ion binding, DNA condensation and structural features. *J. Biomol. Struct. Dynam.* **10**, 865-877.

Thomson, J. B. & Lilley, D. M. (1999). The influence of junction conformation on RNA cleavage by the hairpin ribozyme in its natural junction form. *RNA,* **5**, 180-187.

Topal, M. D. & Fresco, J. R. (1980). Fluorescence of terbium ion-nucleic acid complexes: a sensitive specific probe for unpaired residues in nucleic acids. *Biochemistry,* **19**, 5531-5537.

Tung, C. S., Harvey, S. C. & McCammon, J. A. (1984). Large-amplitude bending motions in phenylalanine transfer RNA. *Biopolymers,* **23**, 2173-2193.

Walter, N. G. & Burke, J. M. (1997). Real-time monitoring of hairpin ribozyme kinetics through base-specific quenching of fluorescein-labeled substrates. *RNA,* **3**, 392-404.

Walter, N. G. & Burke, J. M. (1998). The hairpin ribozyme: structure, assembly and catalysis. *Curr. Opin. Chem. Biol.* **2**, 24-30.

Walter, N. G., Hampel, K. J., Brown, K. M. & Burke, J. M. (1998). Tertiary structure formation in the hairpin ribozyme monitored by fluorescence resonance energy transfer. *EMBO J.* **17**, 2378-2391.

Walter, N. G., Burke, J. M. & Millar, D. P. (1999). Stability of hairpin ribozyme tertiary structure is governed by the interdomain junction. *Nature Struct. Biol.* **6**, 544-549.

Wedekind, J. E. & McKay, D. B. (1998). Crystallographic structures of the hammerhead ribozyme: relationship to ribozyme folding and catalysis. *Annu. Rev. Biophys. Biomol. Struct.* **27**, 475-502.

Welch, P. J., Hampel, A., Barber, J., Wong-Staal, F. & Yu, M. (1996). Inhibition of HIV replication by the hairpin ribozyme. *Nucl. Acids Mol. Biol.* **10**, 315-327.

Wenzel, T. J. & Collette, L. M. (1988). Lanthanide ions as luminescent chromophores for the liquid chromatographic detection of polynucleotides and nucleic acids. *J. Chromatog.* **436**, 299-307.

Wincott, F., DiRenzo, A., Shaffer, C., Grimm, S., Tracz, D., Workman, C., Sweedler, D., Gonzalez, C., Scaringe, S. & Usman, N. (1995). Synthesis, deprotection, analysis and purification of RNA and ribozymes. *Nucl. Acids Res.* **23**, 2677-2684.

Yarus, M. (1993). How many catalytic RNAs? Ions and the Cheshire cat conjecture. *FASEB J.* **7**, 31-39.

Yonuschot, G., Helman, D., Mushrush, G., Woude, G. V. & Robey, G. (1978). Terbium as a solid-state probe for RNA. *Bioinorg. Chem.* **8**, 405-418.

Young, K. J., Gill, F. & Grasby, J. A. (1997). Metal ions play a passive role in the hairpin ribozyme catalysed reaction. *Nucl. Acids Res.* **25**, 3760-3766.

Edited by J. Doudna

(Received 12 January 2000; received in revised form 14 March 2000; accepted 14 March 2000)